symmetry

MDPI

Article

Thermal Conductivity Study of an Orthotropic Medium Containing a Cylindrical Cavity

Ibrahim Abbas [1,2], Marin Marin [3,*], Aatef Hobiny [2] and Sorin Vlase [3,4,*]

[1] Mathematics Department, Faculty of Science, Sohag University, Sohag 82524, Egypt
[2] Mathematics Department, Faculty of Science, King Abdulaziz University, Jeddah 21521, Saudi Arabia
[3] Department of Mathematics and Computer Science, Transilvania University of Brasov, 500036 Brasov, Romania
[4] Romanian Academy of Technical Sciences, B-dul Dacia 26, 030167 Bucharest, Romania
* Correspondence: m.marin@unitbv.ro (M.M.); svlase@unitbv.ro (S.V.)

Abstract: An interesting feature that appears in the thermoelastic interaction in an orthotropic material containing cylindrical cavities is addressed in this study. For this purpose, the Finite Element Method is applied to analyze a generalized thermoelasticity theory with a relaxation time. For the development of the model, a thermal conductivity that is dependent on the temperature of the orthotropic medium was considered. The boundary condition for the internal surface of a cylindrical hollow is defined by the thermal shocks and the traction on the free surface. The nonlinear formulations of thermoelastic based on thermal relaxation time in orthotropic mediums are abbreviated using the Finite Element Method. The nonlinear equations without Kirchhoff's transformations are presented. The results are graphically represented to demonstrate how changing thermal conductivity affects all physical values.

Keywords: thermal relaxation; orthotropic medium; cylindrical cavity; FEM; constitutive law

Citation: Abbas, I.; Marin, M.; Hobiny, A.; Vlase, S. Thermal Conductivity Study of an Orthotropic Medium Containing a Cylindrical Cavity. *Symmetry* **2022**, *14*, 2387. https://doi.org/10.3390/sym14112387

Academic Editors: Vasilis K. Oikonomou and Victor A. Eremeyev

Received: 29 September 2022
Accepted: 8 November 2022
Published: 11 November 2022

1. Introduction

In solid mechanics and material science, an orthotropic media possesses material properties at specified points that change along the three perpendicular axes, each having twofold rotational symmetry. Over the last four decades, a number of mathematicians and engineers have exhibited a great deal of interest in generalized thermoelastic theories because of their remarkable realistic implications in a range of domains, such as acoustics, continuum mechanic, nuclear engineering, aeronautic, high-energy particle accelerator, and so on.

Biot [1] developed the coupled thermoelastic hypothesis to overcome the inconsistency appearing by the uncoupled hypothesis. In this theory, the heat transport and elasticity formulations are coupled. Lord and Shulman [2] proposed many extensions of the thermoelastic theory. In 1980, Dhaliwal and Sherief [3] modified the Lord and Shulman model to include anisotropic cases. Singh [4] has explored the wave propagation in porous materials using thermoelastic models in general. Alesemi [5] used the LS model under the influence of centrifugal force and Coriolis to investigate the plane waves in magneto-thermoelasticity anisotropic materials. Marin et al. [6] presented some results in the Green and Lindsay model of thermoelastic structures. Abouegal et al. [7] have studied the effects of varying properties and rotations in visco-thermoelastic orthotropic cylinders. Biswas [8] studied the surface waves in porous nonlocal orthotropic thermoelastic materials. Abd-Alla et al. [9–11] have discussed the propagations of Rayleigh wave in a generalized thermo-magneto-elasticity orthotropic medium under gravity field with initial stresses. Biswas and Mukhopadhyay [12] have used the eigenfunction expansion approach to analyze thermal shocks behaviors in thermoelastic orthotropic media by using three thermoelastic models with a magnetic field. Demirdžić et al. [13] have applied the

finite volumes method of stress and deformations in thermo-hygro-elastic orthotropic materials. Biswas et al. [14] have applied the TPL model to investigate the Rayleigh surface wave propagations in orthotropic thermoelastic solids. Ding et al. [15] have investigated the solutions of an axisymmetric plane strain dynamics thermoelastic problem with a non-homogeneous orthotropic cylindrical shell.

Green–Naghdi III was utilized by Kaur and Lata [16] to explore the axisymmetric deformations in a transversely isotropic magneto-thermoelastic solid with inclined stress. Biswas and Mukhopadhyay [17] have discussed the Rayleigh waves propagations in orthotropic mediums with phase delays via the eigenfunction expansion technique. Abbas and Zenkour [18] have applied the Green and Naghdi theorem to investigate the effects of rotations and initial stresses in the fiber-reinforced anisotropic. Kar and Kanoria [19] have discussed the three-phase lag (TPL) effect in a thermos-elastic FG orthotropic spheres. The impact of thermal relaxation times on thermal interactions in an infinite orthotropic media containing cylindrical holes was studied by Abbas and Abd-alla [20]. Biswas et al. [21] examined the thermal shock responses in a magneto-thermal orthotropic medium by using the TPL theory. Rayleigh wave in a porous non-local orthotropic layer resting over a porous non-local orthotropic thermoelastic half-space was explored by Biswas [22]. Mondal and Sur [23] have investigated photo-thermoelastic wave propagation and memory responses in orthotropic semiconductors with spherical cavities. Hobiny and Abbas [24] investigated the generalized thermoelasticity interactions generated by a pulse heating transfer in a two-dimensional orthotropic material. Alzahrani et al. [25] applied the eigenvalue method for two-dimension porous materials under weak, strong, and normal thermal conductivity. Sharma et al. [26] discussed the diffusivity and thermal conductivity of a two-temperature thermoelastic diffusions plate under varying thermal conductivity. Abbas et al. [27] have studied the photothermal interaction in semiconductors medium containing a cylindrical cavity and varying thermal conductivity. Said [28] compared three theories using the eigenvalue technique to a problem of magneto-thermoelastic spinning media with changing thermal conductivity. Abbas et al. [29] have applied the finite element approach to study thermoelastic interactions in a polymeric orthotropic material. Zenkour and Abbas [30] have studied the nonlinear transient's thermal stresses analysis of temperature-dependences cylinders by the finite element method. Abbas and Kumar [31] have studied two-dimensional deformations in thermoelastic half-space with voids under initially stress. Kaur and Lata [32] have investigated the impacts of variable thermal conductivity in an isotropic thermoelastic material with modified couple stress under two temperatures. Lata and Kaur [33] have studied the thermal and mechanical interaction in a thermoelastic transversely isotropic solid under a magnetic field with two temperatures and without energy dissipations. Lata et al. [34] have presented the plane waves in anisotropic thermoelastic mediums. Othman et al. [35] have used the TPL model to investigate the effects of rotation in micropolar thermoelastic mediums with voids. Lata and Singh [36] have investigated the deformation in nonlocal magneto-thermoelastic mediums under hall current due to normal forces. Sarkar et al. [37] investigated the effects of a laser pulse on transient waves in thermoelastic material under non-local Green and Naghdi models. Abo-Dahab and Abbas [38] studied the Lord and Shulman theory in thermal shock problems of magneto-thermoelastic with varying thermal conductivity. Alzahrani [39] studied the impact of variable thermal conductivity in semiconducting material. Zenkour et al. [40] have investigated the magneto-thermoelastic responses in unbounded media with spherical cavities under thermoelastic models. Abo-Dahab et al. [41] investigated the generalized thermoelastic FG beam. Numerous researches have been conducted using the generalized thermoelasticity models in the following kinds of literatures [42–51].

This work is devoted to the study of the impacts of varying thermal conductivity in orthotropic medium with cylindrical cavities under thermal shock. Using the finite element methods, numerical solutions for the investigated fields have been produced. The outcomes are then shown visually. The findings of the numerical analysis show that the

variable thermal conductivity gives both mechanical waves and thermal waves a finite velocity of propagation.

2. Basic Equations

Considering an orthotropic material, using the basic formulations under generalized thermoelastic theory [3] without body force and heating source, the equations of motion can be presented as:

$$\sigma_{ij,j} = \rho \frac{\partial^2 u_i}{\partial t^2} \tag{1}$$

where u_i are the displacement components, σ_{ij} are the stress components, and ρ is the mass density. The stress–strain temperature equations are expressed as:

$$\sigma_{ij} = c_{ijkl} e_{kl} - \gamma_i (T - T_o) \delta_{ij} \tag{2}$$

where γ_i are the thermal moduli, T is the temperature increment, T_o is the reference temperature, c_{ijkl} are the elastic constants, and e_{kl} are the strain tensor components. The heat equation according generalized thermoelastic model can be expressed by:

$$\frac{\partial T_{,ii}}{\partial t} \left(K_{jj} T_{,j} \right)_{,j} = \left(1 + \tau_o \frac{\partial}{\partial t} \right) \left(\rho c_e \frac{\partial T}{\partial t} + \gamma_{jj} T_o \frac{\partial u_{j,j}}{\partial t} \right) \tag{3}$$

where K_{jj} are the thermal conductive components, which are affected by temperature and may be varied, and c_e is the specific heat. Consider an elastic unbounded medium containing a cylindrical hole occupying the area $R \leq r < \infty$ as in Figure 1, whose state can be defined in terms the time variable t and the space variable r. The one component that does not vanish is the radial displacement component $u_r = u(r, t)$, which is associated to the cylindrical coordinates (r, θ, z).

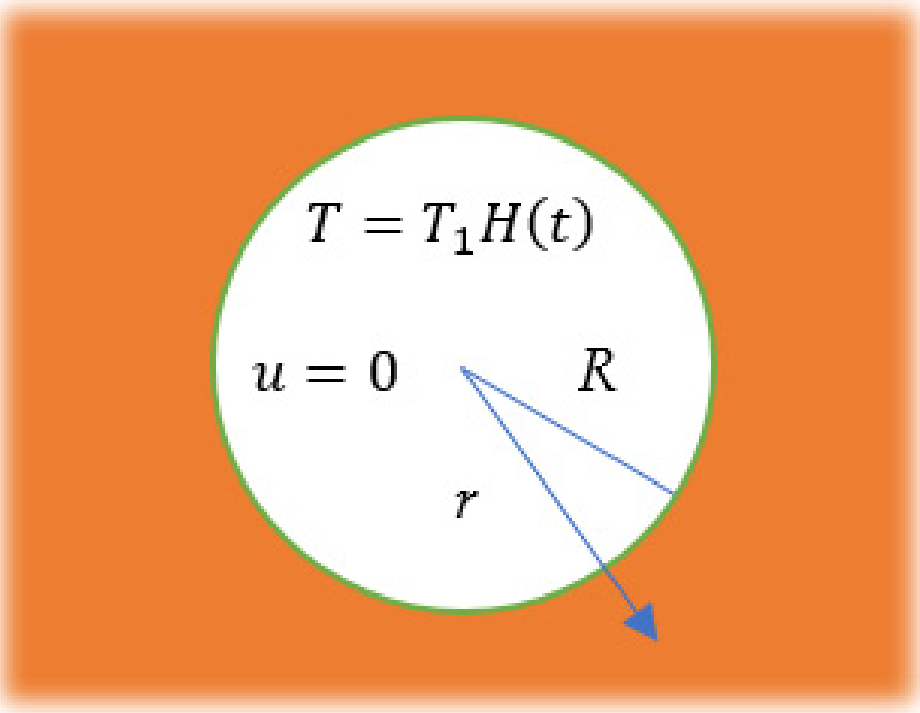

Figure 1. The sketch of an unbounded material containing a cylindrical hole.

The non-vanishing components of the strain tensor by:

$$e_{rr} = \frac{\partial u}{\partial r}, e_{\theta\theta} = \frac{u}{r} \tag{4}$$

Substituting for e_{rr}, $e_{\theta\theta}$ into the basic equations one obtains:

$$\begin{bmatrix} \sigma_{rr} \\ \sigma_{\theta\theta} \end{bmatrix} = \begin{bmatrix} c_{11} \\ c_{12} \end{bmatrix} \frac{\partial u}{\partial r} + \begin{bmatrix} c_{12} \\ c_{22} \end{bmatrix} \frac{u}{r} - \begin{bmatrix} \gamma_{11} \\ \gamma_{22} \end{bmatrix} T \tag{5}$$

$$\frac{\partial \sigma_{rr}}{\partial r} + \frac{1}{r}(\sigma_{rr} - \sigma_{\theta\theta}) = \rho \frac{\partial^2 u}{\partial t^2} \tag{6}$$

$$\frac{1}{r}\frac{\partial}{\partial r}\left(rK(T)\frac{\partial T}{\partial r}\right) = \left(\frac{\partial}{\partial t} + \tau_o \frac{\partial^2}{\partial t^2}\right)\left(\rho c_e T + \gamma_{11} T_o \frac{\partial u}{\partial r} + \gamma_{22} T_o \frac{u}{r}\right) \tag{7}$$

In this situation, the variable thermal conductivity for the orthotropic medium that may be created can be selected as an exponential function of temperature [52].

$$K(T) = K_o e^{K_s T} \tag{8}$$

where K_o are the component of thermal conductivity when $T = T_o$ and $K_s \leq 0$ is the negative parameter.

3. Application

The initial conditions are described by:

$$u(r,0) = 0, \frac{\partial u(r,0)}{\partial t} = 0, \; T(r,0) = 0, \frac{\partial T(r,0)}{\partial t} = 0 \tag{9}$$

While the boundary conditions are expressed by following:

$$T(R,t) = T_1 H(t), u(R,t) = 0 \tag{10}$$

where T_1 is constant and $H(t)$ denotes the Heaviside unit step function. The non-dimensional parameters may be defined by:

$$\left(t^{\circ}, \tau_o^{\circ}\right) = \omega c^2 (t, \tau_o), \; T^{\circ} = \frac{T - T_o}{T_o}, \; \left(\sigma_{rr}^{\circ}, \sigma_{\theta\theta}^{\circ}\right) = \frac{(\sigma_{rr}, \sigma_{\theta\theta},)}{c_{11}}, \left(r^{\circ}, u^{\circ}\right) = \omega c(r,u) \tag{11}$$

where $\omega = \frac{\rho c_e}{K_o}$ and $c^2 = \frac{c_{11}}{\rho}$. The basic formulations for the non-dimensional parameters in Equation (11) are (after removing the superscript $^{\circ}$ for suitability):

$$\begin{bmatrix} \sigma_{rr} \\ \sigma_{\theta\theta} \end{bmatrix} = \begin{bmatrix} 1 \\ f_1 \end{bmatrix} \frac{\partial u}{\partial r} + \begin{bmatrix} f_1 \\ f_3 \end{bmatrix} \frac{u}{r} - \begin{bmatrix} f_2 \\ f_4 \end{bmatrix} T \tag{12}$$

$$\frac{\partial^2 u}{\partial r^2} + \frac{1}{r}\frac{\partial u}{\partial r} - f_3 \frac{u}{r^2} - f_2 \frac{\partial T}{\partial r} + \frac{f_4 - f_2}{r} T = \frac{\partial^2 u}{\partial t^2} \tag{13}$$

$$e^{K_s T}\frac{\partial^2 T}{\partial r^2} + e^{K_s T}\frac{1}{r}\frac{\partial T}{\partial r} + K_s e^{K_s T}\left(\frac{\partial T}{\partial r}\right)^2 = \left(\frac{\partial}{\partial t} + \tau_o \frac{\partial^2}{\partial t^2}\right)\left(T + f_5 \frac{\partial u}{\partial r} + f_6 \frac{u}{r}\right) \tag{14}$$

where:

$$f_1 = \frac{c_{12}}{c_{11}}, \; f_2 = \frac{\gamma_{11} T_o}{c_{11}}, \; f_3 = \frac{c_{22}}{c_{11}}, \; f_4 = \frac{\gamma_{22 T_o}}{c_{11}}, \; f_5 = \frac{\gamma_{11}}{\omega K_o}, \; f_6 = \frac{\gamma_{22}}{\omega K_o}$$

4. Finite Element Technique

The finite element method (FEM) of nonlinear thermoelastic problem can be readily obtained by the standard process. The temperature T and the component of displacement u are connected to the respective nodal values in the finite element technique by:

$$u = \sum_{j=1}^{n} N_j u_j(t),\ T = \sum_{j=1}^{n} N_j T_j(t) \tag{15}$$

where N represents the shape function and n is the nodes number per element. Using Galerkin procedures, the unknown temperature T, the unknown displacement u, and the accompanying test functions are approximated by the same form functions.

$$\delta u = \sum_{j=1}^{n} N_j \delta u_j,\ \delta T = \sum_{j=1}^{n} N_j \delta T_j \tag{16}$$

We assume that the local coordinates of the master elements are within the range $[1, -1]$. In this problem, the quadratic components in one dimension are written as follows:

$$N_1 = \tfrac{1}{2}(\chi^2 + \chi),\quad N_1 = 1 - \chi^2,\quad N_3 = \tfrac{1}{2}(\chi^2 - \chi) \tag{17}$$

Following are the finite element weak formulations that correspond to Equations (13) and (14):

$$\int_R^L \frac{\partial \delta u}{\partial r}\left(\frac{\partial u}{\partial r}\right)dx + \int_R^L \delta u\left(\frac{\partial^2 u}{\partial t^2} - \frac{1}{r}\frac{\partial u}{\partial r} + f_3\frac{u}{r^2} + f_2\frac{\partial T}{\partial r} - \frac{f_4 - f_2}{r}T\right)dr = \delta u\left(\frac{\partial u}{\partial r}\right)_R^L \tag{18}$$

$$\int_R^L \frac{\partial \delta T}{\partial r}\left(e^{K_s T}\frac{\partial T}{\partial r}\right)dr + \int_R^L \delta T\left(\left(\frac{\partial}{\partial t} + \tau_o\frac{\partial^2}{\partial t^2}\right)\left(T + f_5\frac{\partial u}{\partial r} + f_6\frac{u}{r}\right) - e^{K_s T}\frac{1}{r}\frac{\partial T}{\partial r}\right)dr = \delta T\left(e^{K_s T}\frac{\partial T}{\partial r}\right)_R^L \tag{19}$$

and the unknown variables' time derivatives should be calculated using implicit procedures, in the end.

5. Results and Discussion

For a numerical example, the orthotropic materials can be used as numerical computations. To demonstrate the numerical findings acquired in the preceding sections, we may use the values of the physical constants [53]:

$$c_{12} = 1.65 \times 10^{11}\ (\mathrm{N})(\mathrm{m}^{-2}),\ \rho = 8836(\mathrm{kg})(\mathrm{m}^{-3}),\ c_{22} = 3.581 \times 10^{11}\ (\mathrm{N})\ (\mathrm{m}^{-2})$$
$$K_o = 100(\mathrm{W})(\mathrm{m}^{-1})\left(\mathrm{k}^{-1}\right),\ c_e = 427\ (\mathrm{J})\ \left(\mathrm{kg}^{-1}\right)\ \left(\mathrm{k}^{-1}\right),\ c_{11} = 3.71 \times 10^{11}\ (\mathrm{N})\ (\mathrm{m}^{-2})$$
$$T_o = 298\ (\mathrm{k}),\ \gamma_{11} = 7.04 \times 10^6(\mathrm{N})(\mathrm{m}^{-2})\left(\mathrm{k}^{-1}\right),\ \tau_o = 0.05, t = 0.5,\ R = 1$$
$$\gamma_{22} = 6.9 \times 10^6\ (\mathrm{N})\ (\mathrm{m}^{-2})\ \left(\mathrm{k}^{-1}\right)$$

Based on the data above, Figures 2–9 depict the numerical computations of variables over the radial distance r for the generalized thermoelastic model with one thermal relaxation time. The variation of temperature T, the displacement variation u, the variations of stresses σ_{rr}, $\sigma_{\theta\theta}$ have been carried out by taking $t = 0.5$. There are considerable changes in the values of all variables under the variable thermal conductivity, according to the data. There are two groups of figures; in the first group, Figures 2–5 show the variation of temperature T, the displacement variations u, and the variations of radial and hoop stress components σ_{rr}, $\sigma_{\theta\theta}$ along the radial distances r under difference values of variable thermal conductivity when the thermal relaxation time remains constant. In the second group, Figures 6–9 show the temperature variation T, the variations of displacement u, and the variations of radial and hoop stresses components σ_{rr}, $\sigma_{\theta\theta}$ via the radial distances r with thermal relaxation time (the Lord and Shulman model LS) and without thermal relaxation time (the coupled thermoelastic model CT) when the value of the variable ther-

mal conductivity remains constant. Figure 2 displays the temperature variations along the radial distances r. It is seen that it has maximum value $T = 1$ near the cavity's interior surface according to the problem's boundary conditions, and then declines steadily as the radial distance r approaches zero. Figure 3 shows the radial displacement variations via the radial distance. The displacement achieves its largest negative values near the surface, then gradually reaches maximum values close to the surface, and eventually drops to zero. Figure 4 depicts the variation of radial stress σ_{rr} versus the radials distance r. It is clear that it immediately begins from zero and drops to zero to comply with the problem boundary conditions. Figure 5 explains the variation of sheer stress component $\sigma_{\theta\theta}$ along the radial distances r. It is evident that the sheer stress begins with the greatest negative value at the inner surface $R = 1$ and then declines progressively with increasing radial distance r until reaching zero. As anticipated, the variable thermal conductivity has a significant impact on the value of all physical quantities. Figure 6 shows the variation of temperature via the radial distance r. It is clear that it has the same value $T = 1$ near the cavity's interior surface according to the problem's boundary conditions, and the thermal relaxation time reduces the value of temperature to finish quickly. Figure 7 displays the variations of radial displacement along the radial distance r. It is seen that the peak values of radial displacement are higher with thermal relaxation time than without thermal relaxation time. Figure 8 displays the variations of radial stress σ_{rr} along the radial distance r. It is seen that the thermal relaxation time has a great effect on the radial stress. Figure 9 shows the variation of sheer stress component $\sigma_{\theta\theta}$ along the radial distance r. It is observed that the thermal relaxation time also has a major impact on the values of sheer stress.

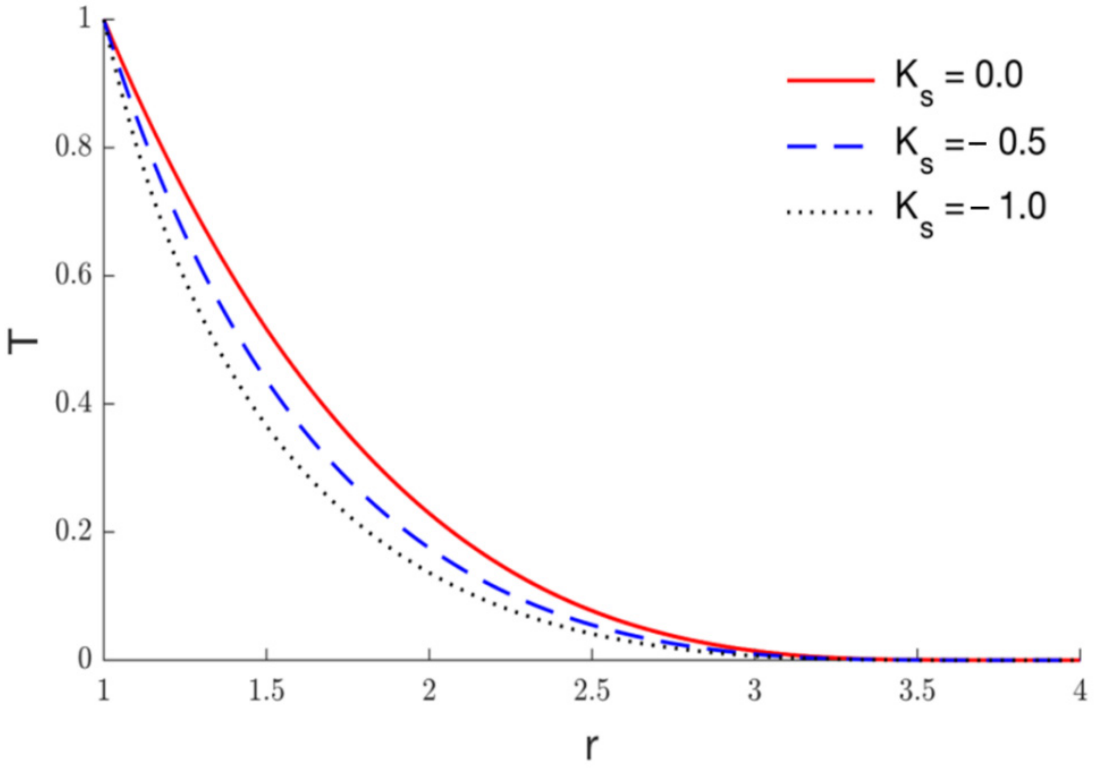

Figure 2. The temperature variation T via the radial distance r under variable thermal conductivity.

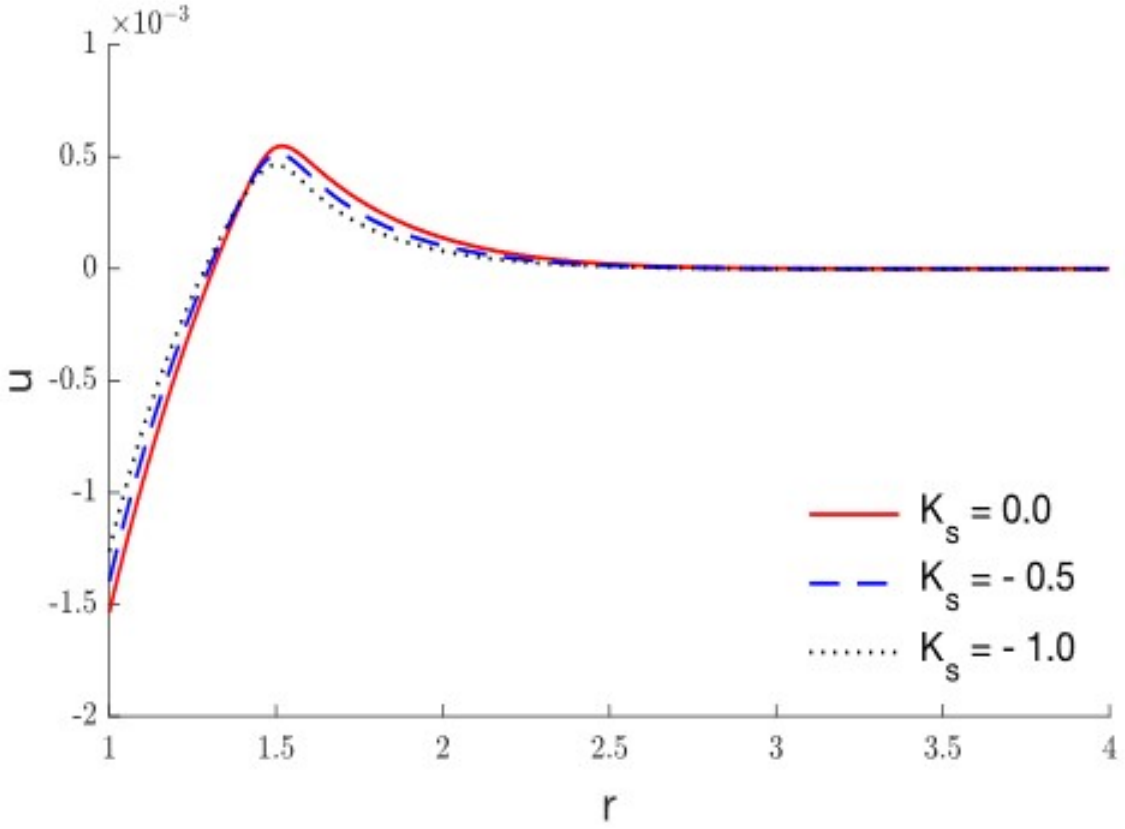

Figure 3. The variations of radial displacement u along the radial distance r under variable thermal conductivity.

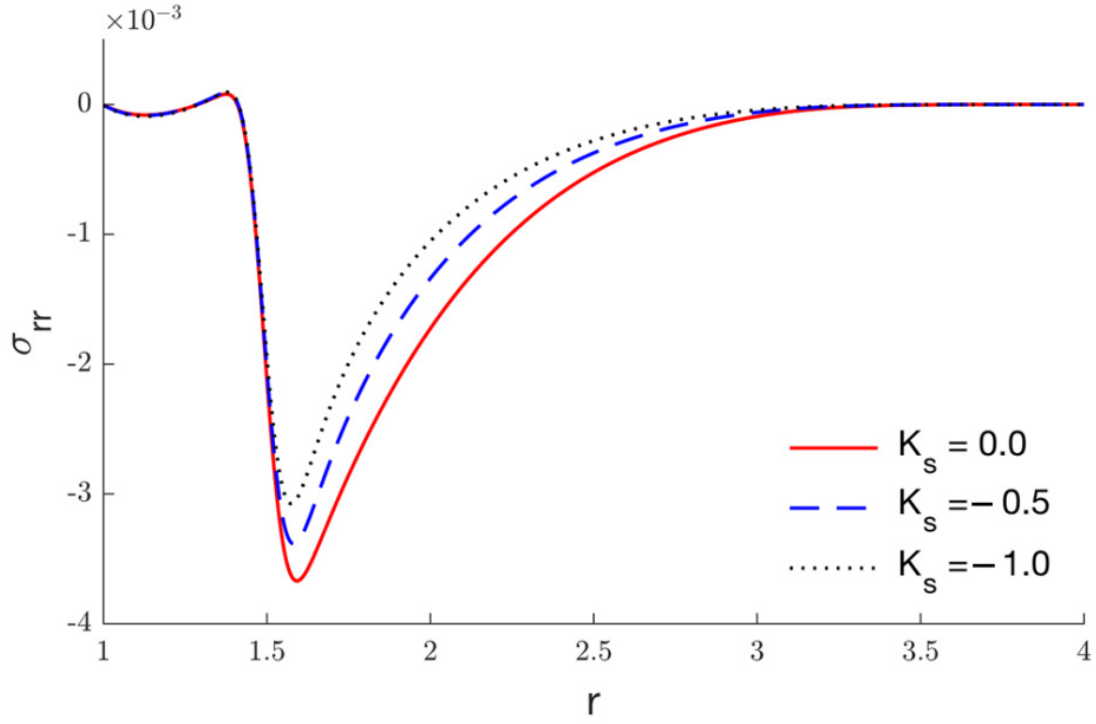

Figure 4. The radial stress variations σ_{rr} via the radial distance r under variable thermal conductivity.

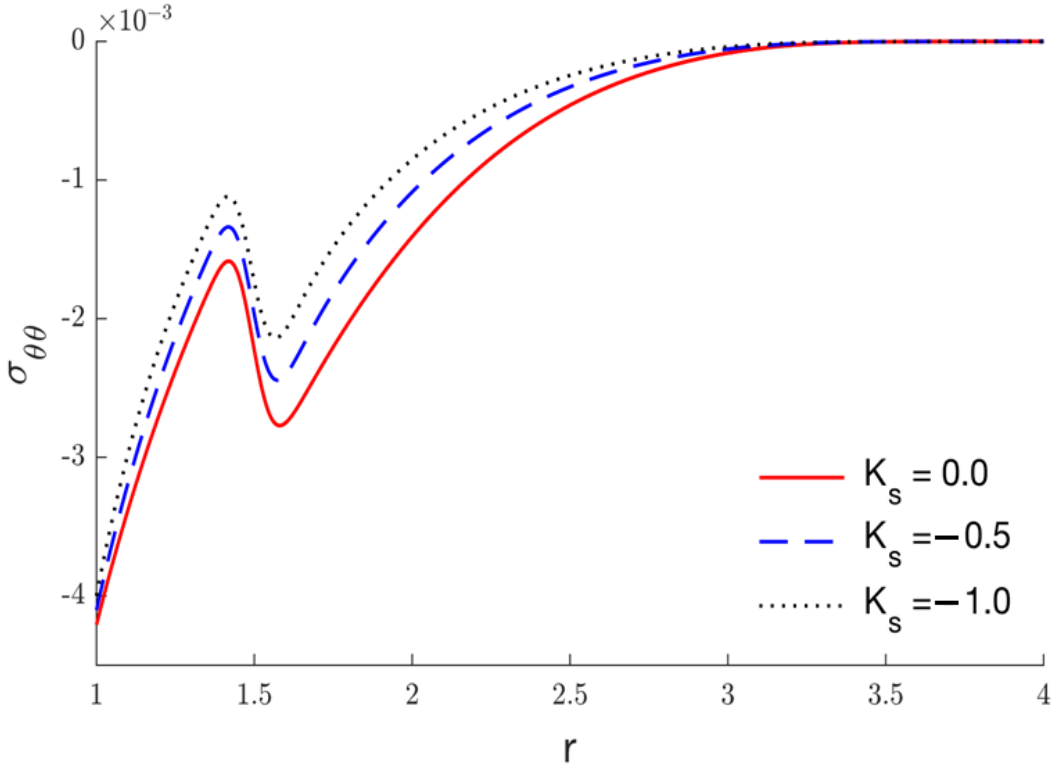

Figure 5. The variations of sheer stress $\sigma_{\theta\theta}$ via the radial distance r under variable thermal conductivity.

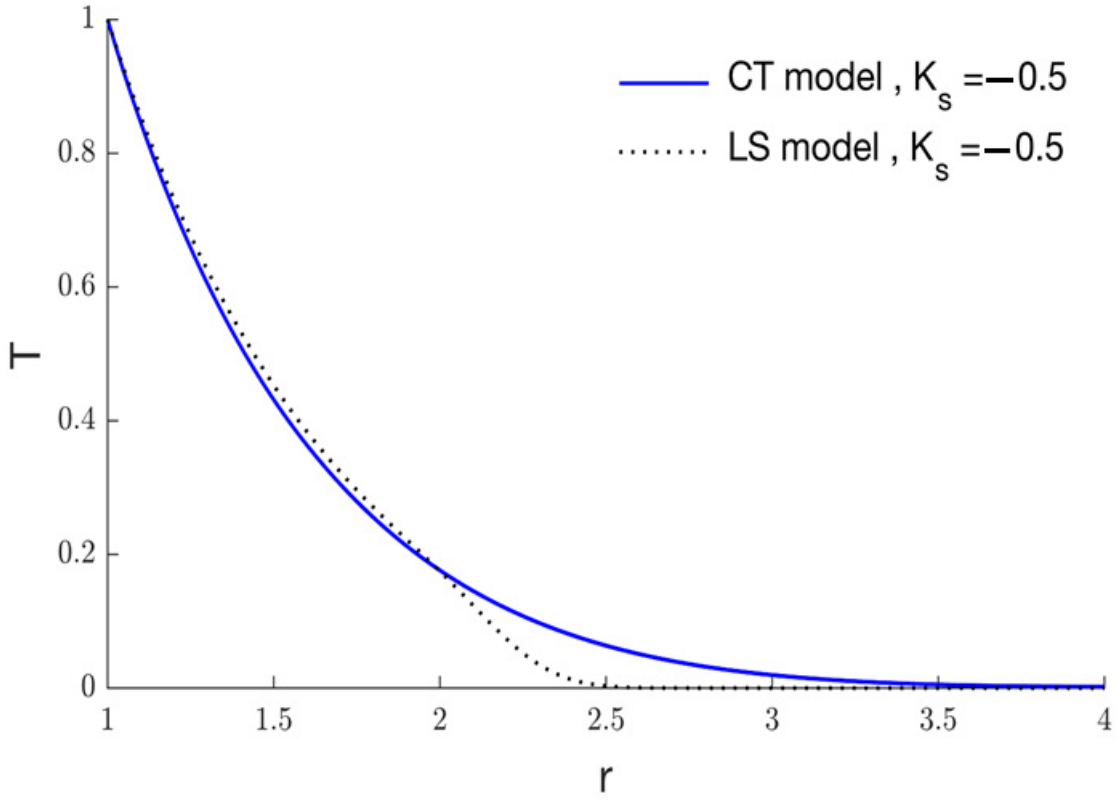

Figure 6. The temperature variation T via the radial distance r under variable thermal conductivity under CT and LS models.

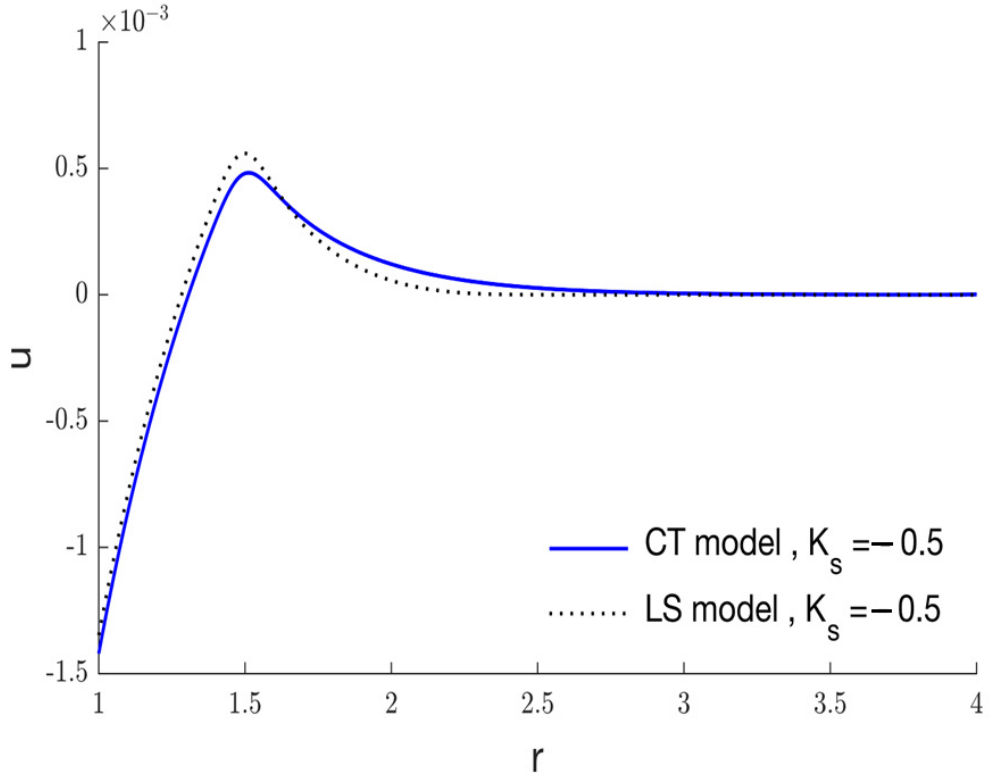

Figure 7. The radial displacement variations u along the radial distance r under variable thermal conductivity under CT and LS models.

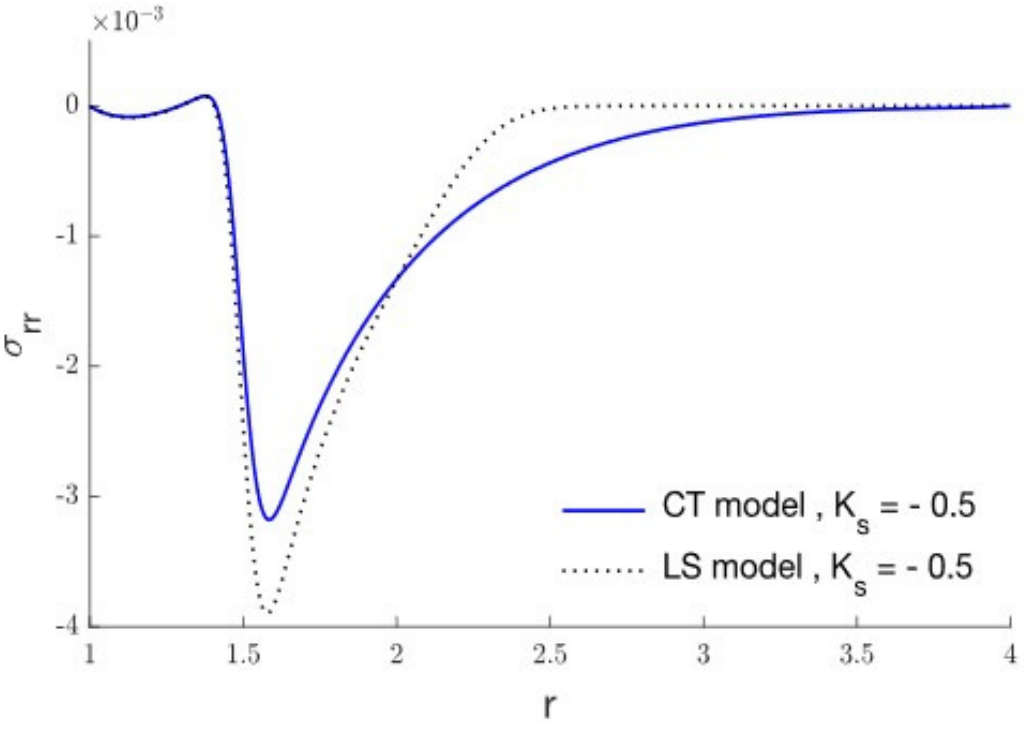

Figure 8. The radial stress variations σ_{rr} along the radial distance r under variable thermal conductivity under CT and LS models.

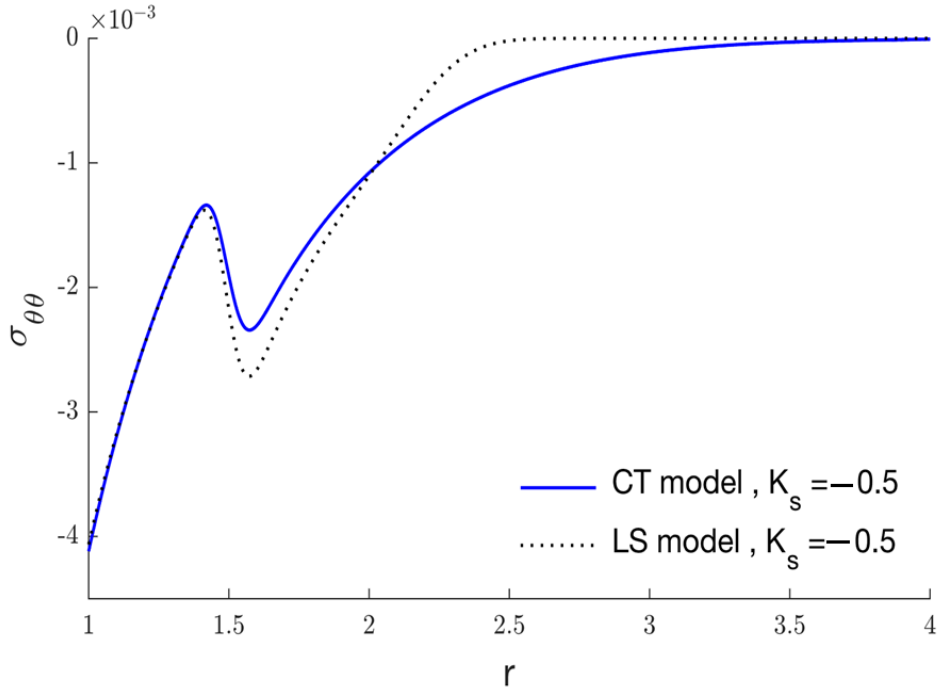

Figure 9. The sheer stress variations $\sigma_{\theta\theta}$ along the radial distance r under variable thermal conductivity under CT and LS models.

6. Conclusions

In this work, the impact of varying thermal conductivity in an orthotropic medium with a cylindrical cavity is mathematically analyzed. Using the thermoelastic model with only one relaxation time, the temperature change, radial displacement, radial distribution, and shear stress distribution in the thermoelastic polymeric orthotropic medium have been presented. The finite element method was applied to get the numerical solution for nonlinear equations. It was determined that the varying thermal conductivity has great impact and plays a role in the behaviors of deformations of different physical field components. Also, the impacts of thermal relaxation time are presented. It was discovered that the thermal relaxation time has a major effect and plays an important role in the behaviors of elastic deformation of different physical field components.

Author Contributions: Conceptualization, I.A. and A.H.; methodology, I.A. and A.H.; software, I.A. and A.H.; validation, I.A., A.H., S.V. and M.M.; formal analysis, I.A., A.H., S.V. and M.M.; investigation, I.A. and A.H.; resources, M.M.; data curation, I.A. and A.H.; writing—original draft preparation, I.A. and A.H.; writing—review and editing, I.A. and A.H.; visualization, I.A., A.H., S.V. and M.M.; supervision, I.A., A.H., S.V. and M.M.; project administration, I.A. and A.H.; funding acquisition, S.V. and M.M. All authors have read and agreed to the published version of the manuscript.

Funding: This research received no external funding. The APC was funded by Transilvania University of Brasov.

Institutional Review Board Statement: Not applicable.

Informed Consent Statement: Not applicable.

Data Availability Statement: Not applicable.

Conflicts of Interest: The authors declare no conflict of interest. The funders had no role in the design of the study; in the collection, analyses, or interpretation of data; in the writing of the manuscript; or in the decision to publish the results.

References

1. Biot, M.A. Thermoelasticity and Irreversible Thermodynamics. *J. Appl. Phys.* **1956**, *27*, 240–253. [CrossRef]
2. Lord, H.W.; Shulman, Y. A generalized dynamical theory of thermoelasticity. *J. Mech. Phys. Solids* **1967**, *15*, 299–309. [CrossRef]
3. Dhaliwal, R.S.; Sherief, H.H. Generalized thermoelasticity for anisotropic media. *Q. Appl. Math.* **1980**, *38*, 1–8. [CrossRef]
4. Singh, B. Wave propagation in a generalized thermoelastic material with voids. *Appl. Math. Comput.* **2007**, *189*, 698–709. [CrossRef]
5. Alesemi, M. Plane waves in magneto-thermoelastic anisotropic medium based on (LS) theory under the effect of Coriolis and centrifugal forces. In *IOP Conference Series: Materials Science and Engineering*; IOP Publishing: Bristol, UK, 2018; p. 012018.
6. Marin, M.; Craciun, E.M.; Pop, N. Some Results in Green–Lindsay Thermoelasticity of Bodies with Dipolar Structure. *Mathematics* **2020**, *8*, 497. [CrossRef]
7. Aboueregal, A.E.; Sedighi, H.M. The effect of variable properties and rotation in a visco-thermoelastic orthotropic annular cylinder under the Moore–Gibson–Thompson heat conduction model. *Proc. Inst. Mech. Eng. Part L J. Mat. Des. Appl.* **2021**, *235*, 1004–1020. [CrossRef]
8. Biswas, S. Surface waves in porous nonlocal thermoelastic orthotropic medium. *Acta Mech* **2020**, *231*, 2741–2760. [CrossRef]
9. Abd-Alla, A.M.; Abo-Dahab, S.M.; Bayones, F.S. Propagation of Rayleigh waves in magneto-thermo-elastic half-space of a homogeneous orthotropic material under the effect of rotation, initial stress and gravity field. *JVC/J. Vib. Control* **2013**, *19*, 1395–1420. [CrossRef]
10. Abd-Alla, A.M.; Abo-Dahab, S.M.; Hammad, H.A.H. Propagation of Rayleigh waves in generalized magneto-thermoelastic orthotropic material under initial stress and gravity field. *Appl. Math. Model.* **2011**, *35*, 2981–3000. [CrossRef]
11. Abd-Alla, A.M.; Abo-Dahab, S.M.; Hammad, H.A.; Mahmoud, S.R. On generalized magneto-thermoelastic rayleigh waves in a granular medium under the influence of a gravity field and initial stress. *JVC/J. Vib. Control* **2011**, *17*, 115–128. [CrossRef]
12. Biswas, S.; Mukhopadhyay, B. Eigenfunction expansion method to analyze thermal shock behavior in magneto-thermoelastic orthotropic medium under three theories. *J. Therm. Stresses* **2018**, *41*, 366–382. [CrossRef]
13. Demirdžić, I.; Horman, I.; Martinović, D. Finite volume analysis of stress and deformation in hygro-thermo-elastic orthotropic body. *Comput. Methods Appl. Mech. Eng.* **2000**, *190*, 1221–1232. [CrossRef]
14. Biswas, S.; Mukhopadhyay, B.; Shaw, S. Rayleigh surface wave propagation in orthotropic thermoelastic solids under three-phase-lag model. *J. Therm. Stresses* **2017**, *40*, 403–419. [CrossRef]
15. Ding, H.J.; Wang, H.M.; Chen, W.Q. A solution of a non-homogeneous orthotropic cylindrical shell for axisymmetric plane strain dynamic thermoelastic problems. *J. Sound Vib.* **2003**, *263*, 815–829. [CrossRef]
16. Kaur, I.; Lata, P. Axisymmetric deformation in transversely isotropic magneto-thermoelastic solid with Green–Naghdi III due to inclined load. *Int. J. Mech. Mater. Eng.* **2020**, *15*, 3. [CrossRef]
17. Biswas, S.; Mukhopadhyay, B. Eigenfunction expansion method to characterize Rayleigh wave propagation in orthotropic medium with phase lags. *Waves Random Complex Media* **2018**, *29*, 722–742. [CrossRef]
18. Abbas, I.A.; Zenkour, A.M. The Effect of Rotation and Initial Stress on Thermal Shock Problem for a Fiber-Reinforced Anisotropic Half-Space Using Green-Naghdi Theory. *J. Comput. Theor. Nanosci.* **2014**, *11*, 331–338. [CrossRef]
19. Kar, A.; Kanoria, M. Generalized thermoelastic functionally graded orthotropic hollow sphere under thermal shock with three-phase-lag effect. *Eur. J. Mech.-A/Solids* **2009**, *28*, 757–767. [CrossRef]
20. Abbas, I.A.; Abd-alla, A.-e.-n.N. Effects of thermal relaxations on thermoelastic interactions in an infinite orthotropic elastic medium with a cylindrical cavity. *Arch Appl Mech* **2007**, *78*, 283–293. [CrossRef]
21. Biswas, S.; Mukhopadhyay, B.; Shaw, S. Thermal shock response in magneto-thermoelastic orthotropic medium with three-phase-lag model. *J. Electromagn. Waves Appl.* **2017**, *31*, 879–897. [CrossRef]
22. Biswas, S. Rayleigh waves in porous nonlocal orthotropic thermoelastic layer lying over porous nonlocal orthotropic thermoelastic half space. *Waves Random Complex Media* **2021**, 1–27. [CrossRef]
23. Mondal, S.; Sur, A. Photo-thermo-elastic wave propagation in an orthotropic semiconductor with a spherical cavity and memory responses. *Waves Random Complex Media* **2020**, *31*, 1835–1858. [CrossRef]
24. Hobiny, A.; Abbas, I. Generalized thermoelastic interaction in a two-dimensional orthotropic material caused by a pulse heat flux. *Waves Random Complex Media* **2021**, 1–18. [CrossRef]
25. Alzahrani, F.; Hobiny, A.; Abbas, I.; Marin, M. An eigenvalues approach for a two-dimensional porous medium based upon weak, normal and strong thermal conductivities. *Symmetry* **2020**, *12*, 848. [CrossRef]
26. Sharma, P.K.; Bajpai, A.; Kumar, R. Analysis of two temperature thermoelastic diffusion plate with variable thermal conductivity and diffusivity. *Waves Random Complex Media* **2021**. [CrossRef]
27. Abbas, I.; Hobiny, A.; Marin, M. Photo-thermal interactions in a semi-conductor material with cylindrical cavities and variable thermal conductivity. *J. Taibah Univ. Sci.* **2020**, *14*, 1369–1376. [CrossRef]
28. Said, S.M. Eigenvalue approach on a problem of magneto-thermoelastic rotating medium with variable thermal conductivity: Comparisons of three theories. *Waves Random Complex Media* **2019**, *31*, 1322–1339. [CrossRef]
29. Abbas, I.; Hobiny, A.; Alshehri, H.; Vlase, S.; Marin, M. Analysis of Thermoelastic Interaction in a Polymeric Orthotropic Medium Using the Finite Element Method. *Polymers* **2022**, *14*, 2112. [CrossRef]
30. Zenkour, A.M.; Abbas, I.A. Nonlinear transient thermal stress analysis of temperature-dependent hollow cylinders using a finite element model. *Int. J. Struct. Stab. Dyn.* **2014**, *14*, 1450025. [CrossRef]

31. Abbas, I.A.; Kumar, R. 2D deformation in initially stressed thermoelastic half-space with voids. *Steel Compos. Struct.* **2016**, *20*, 1103–1117. [CrossRef]
32. Kaur, H.; Lata, P. Effect of thermal conductivity on isotropic modified couple stress thermoelastic medium with two temperatures. *Steel Compos. Struct.* **2020**, *34*, 309–319. [CrossRef]
33. Lata, P.; Kaur, I. Thermomechanical interactions in transversely isotropic magneto thermoelastic solid with two temperatures and without energy dissipation. *Steel Compos. Struct.* **2019**, *32*, 779–793. [CrossRef]
34. Lata, P.; Kumar, R.; Sharma, N. Plane waves in an anisotropic thermoelastic. *Steel Compos. Struct.* **2016**, *22*, 567–587. [CrossRef]
35. Othman, M.I.A.; Alharbi, A.M.; Al-Autabi, A.A.M.K. Micropolar thermoelastic medium with voids under the effect of rotation concerned with 3phl model. *Geomach. Eng.* **2020**, *21*, 447–459. [CrossRef]
36. Lata, P.; Singh, S. Deformation in a nonlocal magneto-thermoelastic solid with hall current due to normal force. *Geomach. Eng.* **2020**, *22*, 109–117. [CrossRef]
37. Sarkar, N.; Mondal, S.; Othman, M.I.A. Effect of the laser pulse on transient waves in a non-local thermoelastic medium under Green-Naghdi theory. *Struct. Eng. Mech.* **2020**, *74*, 471–479. [CrossRef]
38. Abo-Dahab, S.M.; Abbas, I.A. LS model on thermal shock problem of generalized magneto-thermoelasticity for an infinitely long annular cylinder with variable thermal conductivity. *Appl. Math. Model.* **2011**, *35*, 3759–3768. [CrossRef]
39. Alzahrani, F. The effects of variable thermal conductivity in semiconductor materials photogenerated by a focused thermal shock. *Mathematics* **2020**, *8*, 1230. [CrossRef]
40. Zenkour, A.M.; Mashat, D.S.; Allehaibi, A.M. Magneto-Thermoelastic Response in an Unbounded Medium Containing a Spherical Hole via Multi-Time-Derivative Thermoelasticity Theories. *Materials* **2022**, *15*, 2432. [CrossRef]
41. Abo-Dahab, S.M.; Abouelregal, A.E.; Marin, M. Generalized thermoelastic functionally graded on a thin slim strip non-gaussian laser beam. *Symmetry* **2020**, *12*, 1094. [CrossRef]
42. Lata, P.; Singh, S. Stoneley wave propagation in nonlocal isotropic magneto-thermoelastic solid with multi-dual-phase lag heat transfer. *Steel Compos. Struct.* **2021**, *38*, 141–150. [CrossRef]
43. Lata, P. Effect of energy dissipation on plane waves in sandwiched layered thermoelastic medium. *Steel Compos. Struct.* **2018**, *27*, 439–451. [CrossRef]
44. Ezzat, M.A.; El-Bary, A.A. Fractional magneto-Thermoelastic materials with phase-lag Green-Naghdi theories. *Steel Compos. Struct.* **2017**, *24*, 297–307. [CrossRef]
45. Abd-Elaziz, E.M.; Othman, M.I.A. On a magneto-poro-thermoelastic medium under the influence of the Seebeck effect. *Int. J. Numer. Anal. Methods Geomech.* **2019**, *44*, 705–719. [CrossRef]
46. Lata, P.; Kaur, I. Effect of time harmonic sources on transversely isotropic thermoelastic thin circular plate. *Geomach. Eng.* **2019**, *19*, 29–36. [CrossRef]
47. Zhang, L.; Bhatti, M.M.; Michaelides, E.; Marin, M.; Ellahi, R. Hybrid nanofluid flow towards an elastic surface with tantalum and nickel nanoparticles, under the influence of an induced magnetic field. *Eur. Phys. J. Spec. Top.* **2022**, *231*, 521–533. [CrossRef]
48. Abouelregal, A.E.; Marin, M. The size-dependent thermoelastic vibrations of nanobeams subjected to harmonic excitation and rectified sine wave heating. *Mathematics* **2020**, *8*, 1128. [CrossRef]
49. Abouelregal, A.E.; Marin, M. The response of nanobeams with temperature-dependent properties using state-space method via modified couple stress theory. *Symmetry* **2020**, *12*, 1276. [CrossRef]
50. Tiwari, R.; Kumar, R.; Kumar, A. Investigation of thermal excitation induced by laser pulses and thermal shock in the half space medium with variable thermal conductivity. *Waves Random Complex Media* **2022**, *32*, 2313–2331. [CrossRef]
51. Tiwari, R.; Misra, J.C. Magneto-thermoelastic excitation induced by a thermal shock: A study under the purview of three phase lag theory. *Waves Random Complex Media* **2022**, *32*, 797–818. [CrossRef]
52. Sherief, H.H.; Hamza, F.A. Modeling of variable thermal conductivity in a generalized thermoelastic infinitely long hollow cylinder. *Meccanica* **2016**, *51*, 551–558. [CrossRef]
53. Marin, M.; Agarwal, R.P.; Mahmoud, S.R. Nonsimple material problems addressed by the Lagrange's identity. *Bound. Value Probl.* **2013**, *2013*, 135. [CrossRef]